Photon transport effect on intra-subassembly thermal power distribution in fast reactor

Go Chiba*,[a], Masashi Tsuji[a], Tadashi Narabayashi[a]

[a] *Hokkaido University, Kita-ku, Sapporo, Hokkaido 060-8628, Japan*

Abstract

In order to accurately predict intra-subassembly thermal power distribution in a fast reactor, neutron and photon transport calculations are carried out with a multi-purpose reactor physics calculation code system CBZ. All the fission fragment nuclide are treated explicitly during fuel depletion, and irradiation time-dependent energy spectra of delayed fission γ-rays emitted from all the fission fragment nuclides are precisely simulated. Time-dependent delayed β-ray emission and transmutations of fission fragment nuclide by neutron-nuclide reactions are also taken into account. A fuel subassembly model of Japanese prototype fast reactor Monju is used for numerical calculations, and their two-dimensional geometric feature is precisely modeled by a ray-tracing-based collision probability method implemented in CBZ. When the photon transport is considered, total thermal powers in fissile material regions are reduced by about 1.5% except at the beginning of fuel depletion.

Key words: thermal power distribution, fast reactors, photon transport

1. Introduction

Accurate prediction of thermal power spatial distribution in a nuclear fission reactor core is essential for reliable and efficient reactor core designs. In addition to macroscopic spatial power distribution over a whole core required to allocate coolant flow in the core, a microscopic power distribution, *i.e.,* intra-subassemly thermal power distribution, is also important to determine nuclear fuel depletion, neutron irradiation of structure materials and temperature evaluations. In fast reactor core designs, a maximum fuel temperature is one of the most important design parameters and it sometimes restricts a feasible design range.

As well known, nuclear fission reactions release a large amount of energy with some different forms such as kinetic energy of fission fragments, prompt γ- and β-rays, delayed γ- and β-rays emitted from unstable fission fragments. In addition to fission reactions, γ-rays generated by several neutron-nuclide reactions such as (n,γ) and (n,n$'$) reactions also contribute to thermal power generations. Energy given to nuclides by

*Corresponding author, Tel: +81-10-706-6683, Fax: +81-10-706-6683
Email address: go_chiba@eng.hokudai.ac.jp (Go Chiba)

neutron scattering reactions is also not negligible. The simplest way to calculate thermal power distribution coming from these different forms is to determine an effective fission Q-value, Q_f. A thermal power can be obtained by multiplying total number of occurring fission reactions by Q_f. Historically this simple calculation method has been used with some improvement in fast reactor design studies. Its detail is well reviewed in a reference (Hazama, 2013).

In this simple treatment, all the heats generated by a fission reaction are deposited to a medium in which the fission reaction occurs. Actually γ-rays generated by neutron-nuclide reactions and radioactive decay of unstable fission fragments transport in a core and deposit their energy to a medium which is different from a originating medium. This is referred to as a γ-ray (or photon) transport effect on thermal power distribution in the present paper.

Procedure of photon transport effect evaluation is quite simple; one has to calculate γ-ray sources from neutron-nuclide reaction rate distributions, and perform a fixed source photon transport calculation with a particle transport code. Thermal power distribution induced by photons can be obtained from photon flux distribution and the KERMA (Kinetic Energy Release in MAterials) factors of mediums consisting of a reactor core. A reference (Hazama, 2013) reports that the photon transport effect increases heats in fast reactor blanket and shielding regions about 10%. The importance of the photon transport effect has been well recognized and this effect has been taken into consideration somehow in fast reactor core design studies.

Although the photon transport effect can be easily evaluated as above mentioned, there is a difficulty in calculating γ-ray sources originating from radioactive decay of fission fragments: so called the delayed fission γ-rays. Since a strength and energy spectrum of the delayed γ-rays depend on an irradiation profile, they cannot be uniquely determined. In actual calculations of the photon transport effect, however, fission fragment compositions are calculated by assuming an appropriate irradiation condition and a unique delayed γ-ray spectrum per a fission reaction is determined for each fissile nuclide. Then these γ-ray spectra are used commonly during fuel depletion to calculate γ-ray sources. Some have assumed an infinite irradiation since fission fragment compositions can be analytically calculated (Hazama, 2013; Maeda, 2013). This infinite irradiation assumption, however, considers only nuclide transmutations by radioactive decay and cannot treat transmutations by neutron-nuclide reactions.

In the present study, we evaluate the photon transport effect on intra-subassembly thermal power distribution in a fast reactor. A notable point of this study is to rigorously simulate irradiation time-dependent delayed γ-ray sources by simulating explicitly nuclide transmutations of all the fission fragment nuclides by both the radioactive decay and the neutron-nuclide reactions.

2. Numerical calculation procedure

All the numerical calculations are performed with a multi-purpose reactor physics calculation code system CBZ, which is being developed at Hokkaido university. The CBZ code system has been well validated through a post-irradiation examination analysis (Kawamoto, 2012).

2.1. Multi-group neutron and photon libraries

Multi-group neutron and photon libraries are generated from JENDL-4.0 (Shibata, 2011) by the NJOY-99 code (MacFarlane, 2010). The covered energy ranges and the numbers of energy groups are from 10^{-5} eV to 10 MeV and 70 for the neutron library, and from 1 keV to 50 MeV and 42 for the photon library. A lethargy width of all the energy groups except for the final one (from 10^{-5} eV to 0.322 eV) is 0.25 in the neutron library. The energy group structure of the neutron library has been utilized for fast reactor neutronics calculations in Japan. The energy group structure of the photon library is the same as the VITAMIN-J 42-group structure. Options for the weight function choice in NJOY-99 are set to iwt=7 in the neutron library generation and iwt=3 in the photon library generation. Self-shielding factor tables for the neutron library are generated using the narrow resonance approximation for neutron flux representation.

2.2. Treatment of fission fragment nuclide transmutation

Decay data of fission fragment nuclide such as decay constants, decay modes and their branching ratios, decay energy and delayed γ-ray spectra are taken from the JENDL FP Decay Data File 2011 (JENDL/FPD-2011) (Katakura, 2011). The delayed γ-ray spectrum is energy-integrated to the 42-group structure of the photon library. Fission yield data are taken from the JENDL FP Fission Yields Data File 2011 (JENDL/FPY-2011) (Katakura, 2011). We treat all the fission fragment nuclide explicitly in nuclide transmutation calculations. Neutron-nuclide reactions are also considered in the transmutation calculations for 406 nuclides to which the evaluation data are provided in JENDL-4.0. Although neutron-nuclide reaction data are not evaluated for extremely short-lived nuclides in JENDL-4.0, the neutron-nuclide reactions of such nuclides seems negligible in the present heating calculations. The neutron-nuclide reaction rates are obtained in multi-group neutron transport calculations described in the following subsection, and then nuclide transmutation calculations are performed with the matrix exponential method with the Chebyshev rational approximation (Pusa, 2010).

2.3. Neutron and photon transport calculations

We perform neutron and photon transport calculations for a two-dimensional fast reactor fuel subassembly model. The resonance self-shielding effect is evaluated by the method proposed by Tone (Tone, 1975). Whereas the numerical accuracy of this method is inferior to more advanced methods such as the sub-group

method, it has been shown in the previous study that Tone's method can treat spatially-dependent intra-subassembly resonance self-shielding effect of a fast reactor subassembly well (Chiba, 2003). The resonance self-shielding effect is also taken into consideration in γ-ray production cross sections; γ-ray production cross sections are calculated by multiplying the self-shielded neutron-nuclide reaction cross sections by γ-ray yield. The resonance self-shielding calculation is carried out only at the initial depletion step, and the same energy-averaged microscopic cross sections are used in subsequent depletion steps.

After obtaining medium-wise multi-group neutron and photon cross sections, neutron transport calculations are performed by a collision probability-based module of CBZ with an eigenvalue calculation mode. Collision probabilities are calculated by the ray-tracing method with the periodic boundary conditions. The maximum distance between two parallel neighboring rays is 0.01 cm and the azimuthal angle is divided to 48. γ-ray sources promptly emitted from neutron-nuclide reactions are determined from the calculated neutron flux and reaction rate distributions, and then the delayed γ sources emitted from radioactive decay of fission fragments are added to them. Finally a photon transport calculation is performed with the same collision probability-based module of CBZ. In both the neutron and photon transport calculations, the scattering anisotropy is considered by the transport approximation.

2.4. Power distribution calculations

We calculate the following component-wise power distributions.

- The kinetic energy of fission fragments and prompt β-ray energy. The sum of these energy per a fission reaction, E_{FR}, is given in evaluated data files. We use the evaluated data given in JENDL-4.0 for each fissionable nuclide. This power component can be calculated by multiplying total number of fission reactions by E_{FR} for all fissionable nuclides.

- The delayed β-ray energy. This component is calculated from β-ray energy per a radioactive decay, decay constants and number densities of all fission fragment nuclides included in fuel regions.

- The γ-ray energy. This component includes the prompt and delayed fission γ-ray and other neutron-nuclide reaction-induced γ-ray. This component is calculated by multiplying photon flux by the KERMA factor.

- Energy deposited to nuclides by elastic scattering reactions with neutrons. This component is calculated from neutron elastic scattering reaction rates.

In order to evaluate the photon transport effect on thermal power distribution, we also perform a thermal power distribution calculation without considering photon transport. In such calculations, all the γ-ray sources energy is deposited to a medium from which the γ-ray originates.

Note that only emitted γ-ray energy is taken into consideration in inelastic scattering reactions; energy deposited to nuclides by inelastic scattering reactions with neutrons is ignored in the present study.

3. Numerical results

3.1. Validation of nuclide transmutation calculation capability of CBZ

To show a validity of the CBZ capability for nuclide transmutation calculations with over 1,000 fission fragment nuclides, we calculate β- and γ-ray components of plutonium-239 decay heat after burst fission by fast neutrons and compare them with experimental values obtained at Yayoi (Akiyama, 1982). The results are shown in **Figs. 1** and **2**. The experimental values of both the β- and γ-ray components are well reproduced by CBZ and these results are consistent with previous results obtained by Katakura (Katakura, 2011). Thus we can confirm the validity of the nuclide transmutation calculation capability of CBZ.

3.2. Photon transport effect on power distribution

3.2.1. Calculation condition

We evaluate the photon transport effect on thermal power distribution for a fuel subassembly model of Japanese prototype fast reactor Monju. The Monju fuel subassembly is a typical sodium-cooled fast reactor's one; fuel pins are located in a hexagonal array and contained by a stainless-steel wrapper tube. **Figure 3** shows a geometric specification of the Monju fuel subassembly. Some numerical data of the geometric specification are given below.

- subassembly pitch: 11.56 (cm)
- duct (wrapper tube) thickness: 0.3 (cm)
- number of fuel pins in a subassembly: 169
- outer radius of cladding: 0.325 (cm)
- outer radius of fuel pellet: 0.278 (cm)

A gap between fuel pellet and cladding is mixed to the fuel pellet region for simplification in the present calculations. The detail specification can be found in a reference (Takashita, 2000).

The reactor core of Monju consists of two different fuel zones, *i.e.,* inner and outer cores, and the plutonium enrichment of the fuel is different between inner and outer core zones. In the present calculations, we consider these two different fuel compositions. The number densities of fuel pellet, cladding and coolant regions are summarized in **Table 1**. Temperatures of fuel pellet, cladding and coolant regions are set to 1,370, 750 and 750 kelvin, respectively.

In fuel depletion calculations, we assume that the neutron flux level is constant during fuel depletion. Averaged neutron flux levels in fuel regions are set to 3.7×10^{15} and 3.1×10^{15} [/cm^2·s] for inner and outer core subassemblies, respectively. Time steps at which intra-subassembly thermal power distribution is calculated are 0.01, 0.1, 1.0, 10, 100, 1,000 and 10,000 hours.

3.2.2. Irradiation time-dependent delayed γ-ray energy spectra

Figure 4 shows irradiation time-dependent delayed γ-ray energy spectra in the inner core subassembly. Whereas a little time dependence is observed in the shapes of these energy spectra, effect of this time-dependence of γ-ray spectra seems negligible in actual γ-ray transport calculations.

3.2.3. Irradiation time-dependent thermal power

Figure 5 shows irradiation time-dependent total thermal power and its component of kinetic energy of fission fragments and prompt β-ray energy. **Figure 6** shows other thermal power components of the inner core subassembly: γ-ray energy, elastic scattering reaction energy and delayed β-ray energy. A figure for the outer core subassembly is omitted here since the almost same trend is observed as that for the inner core subassembly. The thermal power is defined as a whole fuel subassembly power per a unit axial length. Total thermal power gradually increases at the beginning of fuel depletion, and it begins to decrease after 100 hours of irradiation. This trend is found commonly in both the inner and outer core subassemblies. The gradual increase in the thermal power at the beginning is due to gradual increases in the delayed γ- and β-ray components. The thermal power decrease after 100 hours of irradiation comes from a fissile nuclide depletion since the constant flux is assumed during the fuel depletion. The γ-ray and the delayed β-ray components also decrease at the end of the fuel depletion since the total number of fission reactions decreases around the time. The elastic scattering reaction component is almost constant during the fuel depletion.

In order to see the effect of neutron-nuclide reactions of fission fragment nuclides on thermal power, a different calculation without considering these reactions is carried out. A change in thermal power is negligible and we can conclude that the neutron nuclide reactions of fission fragments are not important to evaluate the delayed γ- and β-ray contributions to the thermal power in the fast reactor Monju.

3.2.4. Photon transport effect on thermal power distribution

Figure 7 shows the total thermal powers in fissile material regions (fuel pellet regions) which are calculated with/without considering the photon transport and **Table 2** summarizes region-wise thermal powers at the irradiation step of 100 hours. Since consideration of the photon transport makes some of the photon energy deposited to non-fuel mediums, especially to cladding and wrapper tube regions, the total thermal powers in fuel regions becomes smaller. **Figure 8** shows the photon transport effect on total thermal power in the fuel pellet regions, which are defined as a ratio between two total thermal powers in the fuel pellet regions calculated with/without considering the photon transport. Since the delayed γ- and β-ray components are quite small, the photon transport effect takes the smallest value at the beginning of the fuel depletion. Even in this extreme case the power reduction in the fuel pellet regions by considering the photon transport is greater than 1.0%. At the time steps after the irradiation time of 10 hours, the transport effects are around 0.985. This value can be used for Monju core design studies since a thermal full

power is rarely attained at the beginning of actual fast reactor operations. **Figure 9** shows fuel pin-wise photon transport effect on thermal powers of fuel region and of fuel and cladding regions in the inner core subassembly. The photon transport effect is larger in the subassembly peripheral region since the some of the photon energy are deposited to the wrapper tube region and the sodium region outside the wrapper tube.

4. Concluding Remarks

In order to accurately predict intra-subassembly thermal power distribution in a fast reactor, neutron and photon transport calculations have been carried out with a multi-purpose reactor physics calculation code system CBZ. All the fission fragment nuclide have been treated explicitly during fuel depletion, and irradiation time-dependent energy spectra of delayed fission γ-rays emitted from all the fission fragment nuclide have been precisely simulated. Time-dependent delayed β-ray emission and transmutations of fission fragment nuclide by neutron-nuclide reactions have been also taken into account. A fuel subassembly model of Japanese prototype fast reactor Monju has been used for numerical calculations, and their two-dimensional geometric feature has been precisely modeled by a ray-tracing-based collision probability method implemented in CBZ. When the photon transport is considered, total thermal powers in fissile material regions are reduced by about 1.5% except at the beginning of fuel depletion. Reduction of the thermal power is larger in fuel pins around a peripheral region of fuel subassemblies since some of photon energy are deposited to a wrapper tube and its outer regions.

It has been also shown that neutron-nuclide reactions of fission fragment nuclides are negligible in evaluation of the photon transport effect on thermal power. Since the neutron-nuclide reactions are much more important in thermal neutron reactors, the present numerical procedure will be applied to thermal power calculations for thermal reactors in future.

Acknowledgements

The authors are grateful to Dr. Jun-ichi Katakura of Nagaoka University of Technology for his advices throughout this study.

References

Akiyama, M., Furuta, K., Ida, T., Sakata, K., An, S. Measurements of gamma-ray decay heat of fission products for fast neutron fission of ^{235}U, ^{239}Pu and ^{233}U, J. At. Energy Soc. Jpn., 24, 803-816.[in Japanese]

Chiba, G. A combined method to evaluate the resonance self shielding effect in power fast reactor fuel subassembly calculation, J. Nucl. Sci. Technol., 40, 537-543.

Hazama, T., Yokoyama, K. Development of versatile nuclear heating calculation system in MARBLE, J. Nucl. Sci. Technol., 50, 525-533.

209 Katakura, J. JENDL FP decay data file 2011 and fission yields data file 2011, JAEA-Data/Code 2011-025, Japan Atomic
210 Energy Agency.
211 Kawamoto, Y., Chiba, G., Tsuji, M., Narabayashi, T. Validation of CBZ code system for post irradiation examination analysis
212 and sensitivity analysis of (n,γ) branching ratio, Proc. of the 2012 Annual Symposium on Nuclear Data (NDS 2012), Kyoto,
213 Japan, Nov. 15-16, 2012, [to be published].
214 MacFarlane, R. E., Kahler, A. C. Methods for processing ENDF/B-VII with NJOY, Nucl. Data Sheets, 111, 2739-2890.
215 Maeda, S., Naito, H., Soga, T., Aoyama, T. Gamma heat rate evaluation for material irradiation test in the experimental fast
216 reactor Joyo, Proc. of Int. Conf. of Nuclear Data for Science and Technology, ND2013, New York, NY, March 4-8, 2013, [to
217 be published].
218 Takashita, H., Higuchi, M., Togashi, N., Hayashi, T. Report on neutronic design calculational methods, JNC TN8410 2000-011,
219 Japan Nuclear Cycle Development Institute. [in Japanese]
220 Pusa, M., Leppänen, J. Computing the matrix exponential in burnup calculations, Nucl. Sci. Eng., 164, 140-150.
221 Shibata, K., Iwamoto, O., Nakagawa, T., Iwamoto, N., Ichihara, A., Kunieda, S., Chiba, S., Furutaka, K., Otuka, N., Ohsawa,
222 T., Murata, T., Matsunobu, H., Zukeran, A., Kamada, S., Katakura, K. JENDL-4.0: a new library for nuclear science and
223 engineering, J. Nucl. Sci. Technol., 48, 1-30.
224 Tone, T. A numerical study of heterogeneity effects in fast reactor critical assemblies J. Nucl. Sci. Technol., 12, 467-481.

Table 1: Nuclide number densities of Monju fuel subassembly

Region	Nuclide	Number density (/barn/cm)	
		Inner core	Outer core
Fuel pellet	Pu-239	2.54335E-03*	3.42379E-03
	Pu-240	1.04803E-03	1.41083E-03
	Pu-241	6.08807E-04	8.19558E-04
	Pu-242	1.73225E-04	2.33190E-04
	U-235	3.09698E-05	2.80175E-05
	U-238	1.52587E-02	1.38041E-02
	O-16	3.84330E-02	3.88474E-02
Cladding	Cr-Nat.	1.70972E-02	
	Fe-Nat.	6.13318E-02	
	Ni-Nat.	1.20286E-02	
	Mn-55	1.42779E-03	
	Mo-Nat.	1.36265E-03	
Coolant	Na-23	2.25394E-02	

* Read as 2.54335×10^{-3}.

Table 2: Region-wise thermal power at t=100 hours (unit: kW/cm)

Region	Inner core		Outer core	
	w Tr.*	w/o Tr.**	w Tr.	w/o Tr.
Fuel pellet	36.664	37.226	38.807	39.389
Cladding	0.504	0.230	0.483	0.196
Wrapper tube	0.348	0.103	0.331	0.139
Sodium inside wrapper tube	0.158	0.083	0.149	0.073
Sodium outside wrapper tube	0.037	0.020	0.035	0.018

* With photon transport, ** Without photon transport

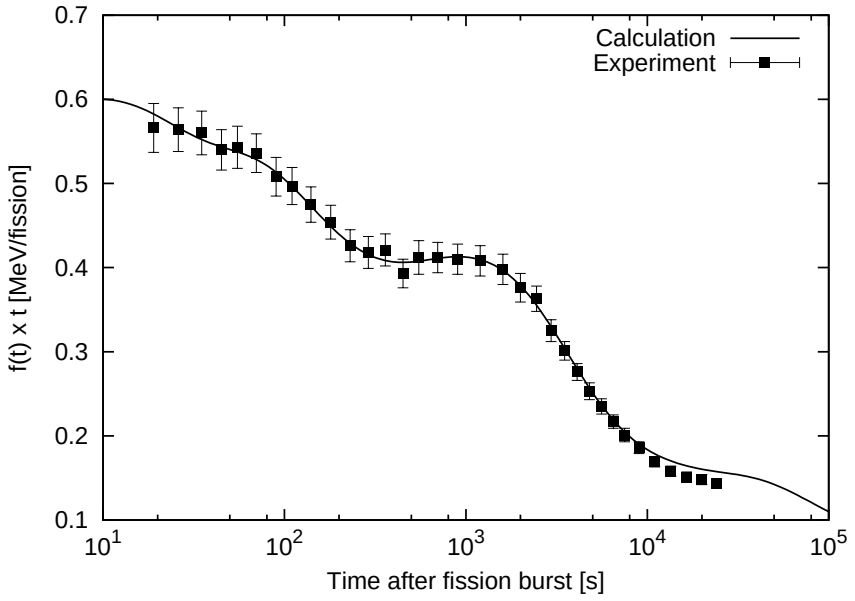

Figure 1: β-ray component of plutonium-239 decay heat after burst fission by fast neutrons

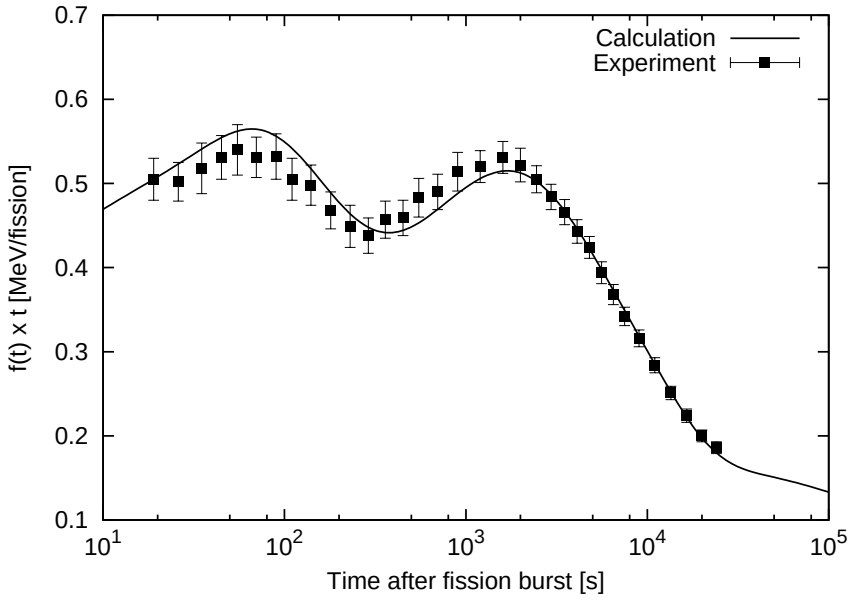

Figure 2: γ-ray component of plutonium-239 decay heat after burst fission by fast neutrons

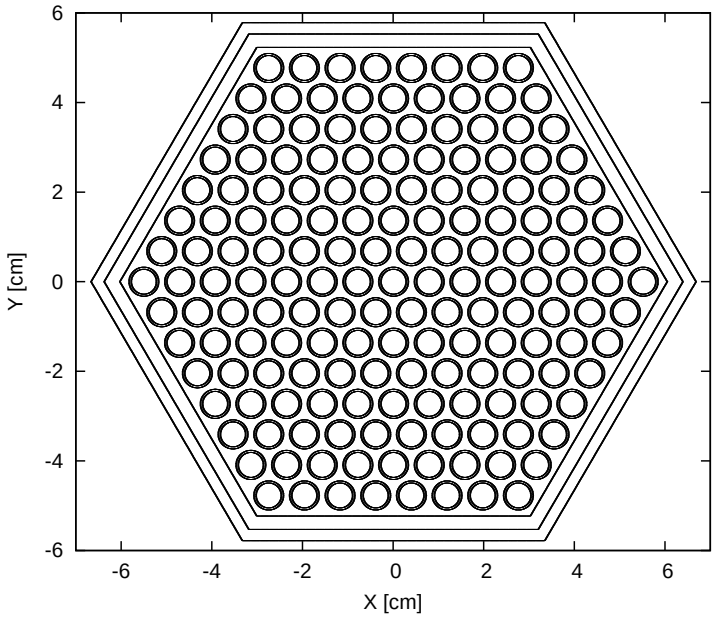

Figure 3: Specification of fuel subassembly of Japanese prototype fast reactor Monju

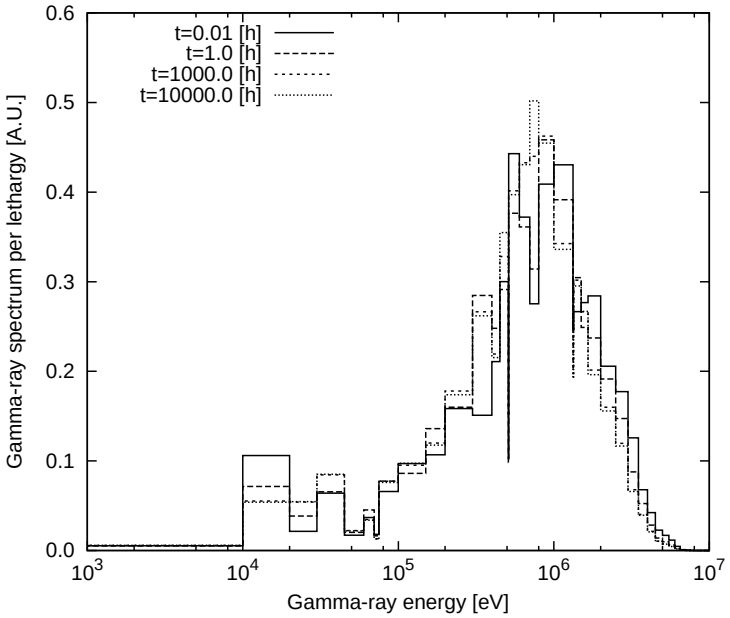

Figure 4: Irradiation time-dependent delayed γ-ray energy spectra

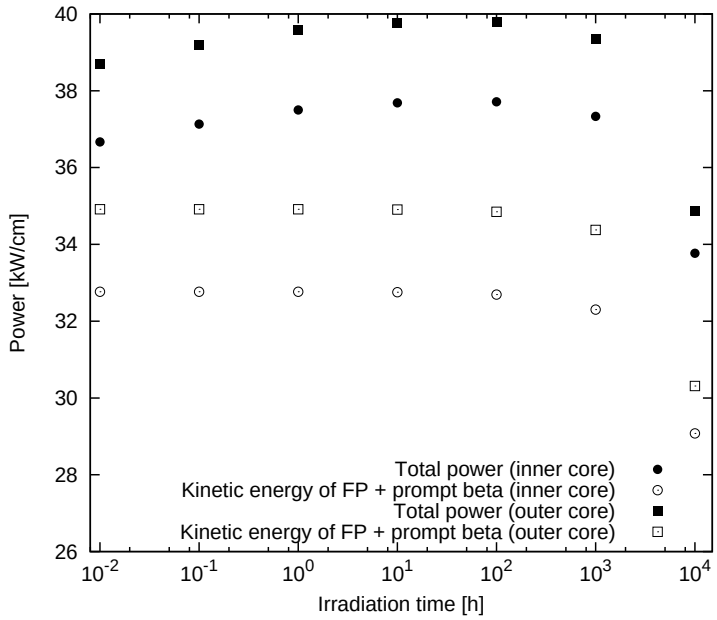

Figure 5: Irradiation time-dependent total thermal power and its component of kinetic energy of fission fragments and prompt β-ray energy

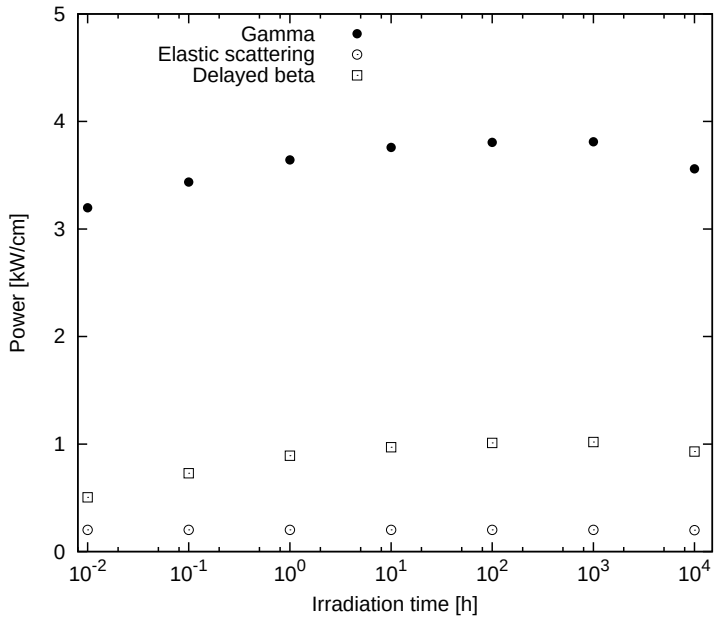

Figure 6: Irradiation time-dependent thermal power components: γ-ray energy, elastic scattering reaction energy and delayed β-ray energy

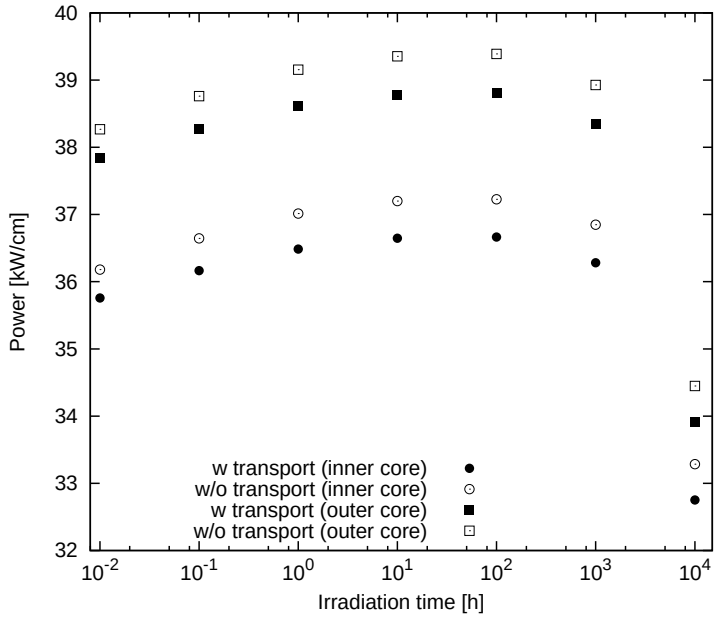

Figure 7: Thermal power in fuel regions with and without consideration of photon transport

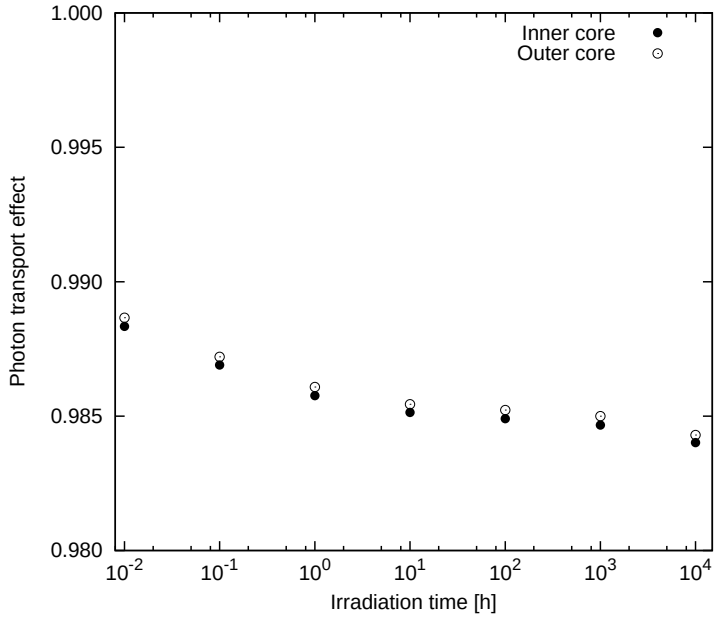

Figure 8: Photon transport effect on thermal power in fuel pellet regions

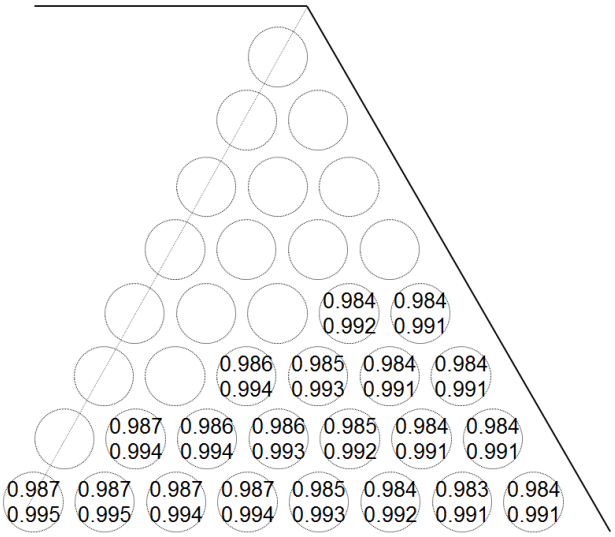

Figure 9: Fuel pin-wise photon transport effect on thermal power of fuel region in inner fuel subassembly (upper: fuel pellet, lower: fuel pellet and cladding)

List of Figure Captions